に理解し，かつ制御できるところにサイエンスの核心があるのではないだろうか．タンパク質を構成するすべての原子の軌道を滑らかに〝見る〟のは至難の業であろう．したがって，このようなところに，21世紀のタンパク質科学の進むべき方向がある，と私は考えている．

参考文献

1) S. B. Prusiner, *Science,* **216**, 136 (1982).
2) S. B. Prusiner, in "Prion biology and diseases," Cold Spring Harbor Press (1999).
3) S. B. Prusiner, *Proc. Natl. Acad. Sci. USA,* **95**, 13363 (1998).
4) 桑田一夫，蛋白質 核酸 酵素，**47**，1292 (2002).
5) C. Weissmann, M. Enari, P. C. Klohn, D. Rossi, E. Flechsig, *Proc. Natl. Acad. Sci. USA,* **99**, 16378 (2002).
6) C. B. Anfinsen, *Harvey Lect.,* **61**, 95 (1967).
7) Y. Zhou, M. Karplus, *Nature,* **23**, 400 (1999).
8) 桑田一夫，数理科学，**43**, 45 (2005).
9) A. M. Odlyzko, *Math. Comp.,* **48**, 273 (1987).
10) K. Kuwata, Y-O. Kamatari, K. Akasaka, T. L. James, *Biochemistry,* **43**, 4439 (2004).
11) G. Legname, I. V. Baskakov, H. O. Nguyen, D. Riesner, F. E. Cohen, S. J. DeArmond, S. B. Prusiner, *Science,* **306**, 673 (2004).
12) M. Fandrich, M. A. Fletcher, C. M. Dobson, *Nature,* **410**, 165 (2001).
13) K. J. Knaus, M. Morillas, W. Swietnick, M. Malone, W. K. Surewicz, V. C. Yee, *Nat. Struct. Biol.,* **8**, 770 (2001).
14) C. Govaerts, H. Wille, S. B. Prusiner, F. E. Cohen, *Proc. Natl. Acad. Sci. USA,* **101**, 8342 (2004).
15) C. S. Burns, E. Aronoff-Spencer, G. Legname, S. B. Prusiner, W. E. Antholine, G. J. Gerfen, J. Peisach, G. L. Millhauser, *Biochemistry,* **42**, 6794 (2003).
16) 桑田一夫，蛋白質核酸酵素，**49**，1110 (2004).

S. B. Prusiner 博士

Stanley B. Prusiner博士は，1942年5月28日に米国で生まれた．現在，カリフォルニア大学サンフランシスコ校医学部神経内科学教授であり，サンフランシスコ在住である．

Prusiner博士は，ヤコブ病の感染因子であるプリオンタンパク質の発見により，1997年，ノーベル生理学医学賞を受賞した．

プリオンタンパク質の異常立体構造が，その正常立体構造と接触することにより，正常立体構造を異常立体構造に変換するというPrusiner博士が提案した大胆な「プリオン仮説」は，長い論争のすえ，ほぼ受け入れられるに至った．それまでにどのような説があったか，まとめると以下のようになる．

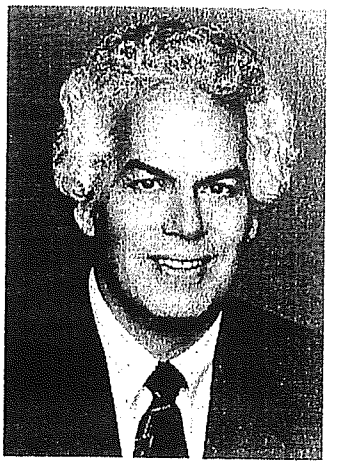

© The Nobel Foundation

プルシナー博士(Stanley B. Prusiner, 1942～　)，カリフォルニア大学サンフランシスコ校医学部神経内科学教授．ヤコブ病の感染因子であるプリオンタンパク質の発見により，1997年，ノーベル生理学医学賞を受賞．

① 寄生虫．
② ウイルス．ネマウイルス．レトロウイルス．(いずれもサイズが大き過ぎた)
③ 細胞膜と結合した多糖類．複製する多糖体．(糖がプリオンの株にかかわっている可能性はあるが，複製する本体とは考えられない)
④ 複製するタンパク質．タンパク質は決して自分だけの力で複製できない．(正常プリオンは，〝立体構造〟の異なる異常プリオンに変化する)
⑤ サブウイルス．ウイリノ．ウイルスよりさらに小さいが，核酸をもつ感染性粒子．(その存在はいまだに実証されていない)
⑥ 裸の核酸．これは植物にあるウイロイドに近いもの．(しかし，核酸は紫外線に弱いが，異常プリオンは紫外線に強いので当てはまらない)
⑦ 多糖体に覆われた核酸．膜と結合したDNA．(核酸は紫外線に弱い．現在に至るまで，プリオン粒子に核酸の存在は確認されていない)
⑧ 線維状ウイルス．(感染性をもつ異常プリオンは，必ずしも線維状ではない)
⑨ アルミニウム-ケイ素-アミロイド複合体．
⑩ コンピュータウイルス〔D. C. Gajdusek, *J. Neuroimmunol.*, **20**, 95 (1998)〕．
⑪ アミロイドを形成するウイルス．
⑫ アポプリオンとコプリオンの複合体(統一理論)．物理学の「統一理論」のアナロジー？

以上の説は，学術雑誌に公表されたものばかりである．これらはすべて否定され，最終的に生き残ったのは，Prusiner博士が唱えた「プリオン仮説」である．この例は，サイエンスの発展を考える際に，非常に示唆的である．サイエンスにおいて，一つの学説が受け入れられるためには，それ以外のありとあらゆる可能性が否定されなければならない．さらに重要なことは，研究者にとって間違った学説を発表する可能性が高いということである．そうならないためにはどうすればよいだろうか．

正しいか正しくないかということは，学説そのものよりもむしろ研究態度の問題である．どのような研究態度が必要なのだろうか．以下にそれを列挙しよう．

① 論理的に説明できない実験操作は決して行わない．
② 行った実験操作は可能なかぎりすべて論文に記載する．
③ 論理はすべて実験的なエビデンスに基づいて展開する．
④ 明快な論理を展開し，飛躍しない．
⑤ 考えられる例外的な可能性をすべてディスカッションに記載する．
⑥ 自説が最終的に証明されるまで一生続ける．

これらが守られるかぎり，どのような大胆な説でも原理的に展開可能である．Prusiner博士の一見，大胆な考え方が受け入れられている背景にはこのような基礎的事項の遵守がある．もちろん，展開されるべき論理が現在のサイエンスの理論的水準で考えて納得可能なものでなければならないことはいうまでもない．この納得可能な線を知るために，現代の自然科学を支える数学や物理学の内部構造に対する理解が必要となる．

現代のタンパク質科学は，数学，物理学，化学，生物学，そして医学を含む総合的な学問体系である．そこではそれぞれの学問の垣根を越えて，最先端の概念が結びつかないと解決できないようなプリオン機構に絡む複雑な問題が存在している．若い人の果敢なチャレンジを期待したい．　　（桑田　一夫）

Semi-classical Quantization of Protein Dynamics: Novel NMR Relaxation Formalism and its Application to Prion

Kazuo Kuwata

Division of Prion Research, Center for Emerging Infectious Diseases, Gifu University, 1-1 Yanagido, Gifu 501-1194, Japan
<e-mail> kuwata@cc.gifu-u.ac.jp

Summary. Novel nuclear spin relaxation mechanism in proteins on a timesclae of micro to milliseconds has been proposed using the Berry-phase interference between periodic orbits within the semi-classical quantization formalism. In order to examine the proposed formalism, susceptibility has been represented by an analytical formulation as a function of the frequency of the periodic orbits, using a Riemann ζ function. Numerically obtained profile of the susceptibility has been quantitatively compared with that of experimentally obtained slow exchange rates in a stable globular protein, $p8^{MTCP1}$ and in a hamster prion protein. Behavior of amide nitrogen atoms in $p8^{MTCP1}$ was almost uniform between residues, and consistent with that of theoretically obtained ones. On the other hand, that of hamster prion was not uniform and quite different than that of theoretical one, suggesting that the slow dynamics of a hamster prion might not be well described by the periodical orbits around the unique saddle point. Local trajectories in the phase space around the native conformation of the hamster prion may be connected to the complicated geometry, corresponding to multiple conformational states, for instance, PrP^C, PrP* or PrP^{Sc}.

Key words. prion, semiclassical quantization, NMR, trace formula, Riemann zeta function

Introduction

Rigorous treatment of the quantization of protein's dynamics may be the critical procedure to understand its biological function. Normal modes at the local phase space around the energy minima representing the dynamics

on the time scale of picoseconds, are relatively well defined. However, we do not have much insight on the geometry of the phase space outside of these integrable harmonic modes. Recent single molecule observation techniques, such as the single channel recording [1], the fluorescence detected single molecular observation in the evanescent field [2], the CPMG relaxation dispersion methods [3,4] strongly indicate that a protein undergoes the very slow fluctuation on a timescale of micro- to milliseconds between a few discrete multiple conformational states. First, we will propose just phenomenological representation of such a phenomenon using a simple kinetic model.

$\Xi_{ji}(t)$ denotes the non-covalent bond interaction energy at site j. Here it is assumed that exchange reaction occurs between conformations i, c.f. A and B:

$$\Xi_{ji}(t) = \begin{cases} \Xi_{jA}(t); when\, the\ protein\ is\ in\ conformation\ A\ at\ time\ t \\ \Xi_{jB}(t); when\, the\ protein\ is\ in\ conformation\ B\ at\ time\ t \end{cases} \quad (1)$$

The expected value for the macroscopic observable, $\Theta_i(t)$ is given by

$$\Theta_i(t) = \sum_{j=1}^{n} \left\langle \Psi_j(t) \middle| O_{ji} \middle| \Psi_j(t) \right\rangle, \quad (2)$$

where

$$\left|\Psi_j(t)\right\rangle = e^{-i\Xi_{jB}(t-t_m)} e^{-i\Xi_{jA}(t_m-t_{m-1})} \cdots e^{-i\Xi_{jB}(t_2-t_1)} e^{-i\Xi_{jA}t_1} \left|\Psi_j(0)\right\rangle \quad (3)$$

and O_{ji} is the observable.

Protein dynamics on a timescale of micro- to milliseconds or thermodynamical stability is directly related to its biological function or its pathogenicity [5]. However, the nature of the slow motion is essentially different than that of the fast motion on a timescale of pico- to nanoseconds. Since the first folding reactions of proteins, such as the prion protein [6], occur within ~100 microseconds at room temperature, the phase trajectories during micro- to milliseconds essentially include the transition between the unfolded and the folded states. CPMG relaxation dispersion measurements [3,4] could elucidate such a dynamics of proteins on a timescale of micro- to milliseconds. In general, slow movements occurring really gradually during micro- to milliseconds can be detected through the changes of the electronic states around nuclei (chemical shifts). However, we cannot exclude the possibility that the fast movements on a timescale of pico- to nanoseconds rarely occurring almost randomly during micro- to milliseconds, because in the NMR relaxation measurements, population changes are essentially observed. On the other hand, accumulated data of single molecular measurements suggest that the former is more realistic. Overall it may be reasonable to assume that slow dynamics is potentially

complicated, recursive, transitive and possibly chaotic [7], and may be characteristic to proteins.

So far magnetic relaxation processes of nuclei in a protein have been interpreted and analyzed based on the linear response theory created by R. Kubo [8] or A.G. Redfield [9]. Although several convenient dynamical models were proposed, such as the model-free system [10], there have been actually no theoretical attempts to include the inherent complexities of the protein dynamics on a timescale of micro to milliseconds. Here we first propose the novel strategy based on the quantization of protein dynamics within a semi-classical approximation, which is then represented by a prime number theory in order to obtain the explicit analytical formulation.

Characteristics of protein dynamics

Protein-water system is generally considered as the typical chaotic system [7] defined by the characteristics of Lyapunov Exponents. In the energy conservation system of degree of freedom s, there are 2n-1 Lyapunov exponents which are positive: ($\lambda_1 = \lambda_2 = \sim = \lambda_q$) or negative ($\lambda_{q+1} = \lambda_{q+2} = \sim = \lambda_{2n-1}$) with $\sum_{i=1}^{2n-1} \lambda_i = 0$. Especially in the Hamilton system, $\lambda_{2n-i+1} = -\lambda_i$.

In such a complex system, we can define the Kolmogorov-Sinai entropy. Phase space is divided into m cells ($i_0, i_1, \ldots i_{m-1}$) with volume δv. If the probability that the trajectory is along the chain of cells is $P_{i0i1\ldots im-1}$, the entropy of the set of trajectories is

$$K_m = -\sum_{i_0 \cdots i_{m-1}} P_{i_0 i_1 \cdots i_{m-1}} \ln P_{i_0 i_1 \cdots i_{m-1}} \tag{4}$$

In the KAM(Kolmogorov-Arnold-Moser) torus, $K_m = 0$, while in chaotic set, entropy generation rate is defined as

$\Delta K_m/\Delta t = (K_m - K_{m-1})/\Delta t$. Then Kolmogorov-Sinai entropy is:

$$h_{KS} = \lim_{\Delta v \to 0} \lim_{\Delta t \to 0} \lim_{N \to \infty} N^{-1} \sum_{m=1}^{N} \Delta K_m / \Delta t = \lim_{\Delta v \to 0} \lim_{\Delta t \to 0} \lim_{N \to \infty} K_N /(N \Delta t) \tag{5}$$

It is known that for periodic motion, $h_{KS} = 0$, for Brownian motion, $h_{KS} = \infty$ and for chaos, $0 < h_{KS} = \infty$. For example, in a protein system (open Hamilton system), it is reported that the Lyapunov exponent > 0 and the KS entropy, $0 < h_{KS} = +\infty$ using molecular dynamics simulation [7].

Gutzwiller's Trace Formula

Let us consider a particle of mass m moving in a d dimensional space. x and y represent the coordinate and the momentum, respectively. Its Hamiltonian is

$$H(x) = -(\hbar^2/2m)\sum_{j=1}^{d} \partial^2/\partial x_j^2 + V(x_1, x_2, \cdots, x_d) \tag{6}$$

and the Schrödinger equation is

$$H(x)\Psi_n(x) = E_n\Psi_n(x). \tag{7}$$

Its solution can be obtained by the following Green function

$$G(x'', x'; E) = \sum_n \Psi_n(x'')\Psi_n(x')/(E - E_n), \tag{8}$$

where E_n can be obtained by summing up the poles of the trace

$$TrG(E) = (\equiv \int dq G(x, x; E)) = \sum_n \frac{1}{E - E_n}. \tag{9}$$

Since

$$(x + i\varepsilon)^{-1} = \wp x^{-1} - i\pi\delta(x), \tag{10}$$

density of state is

$$-\pi^{-1}\,\mathrm{Im}(TrG(E)) = \sum_n \delta(E - E_n)(\equiv \rho(E)) \tag{11}$$

On the other hand, Green function is the Laplace transformation of the propagator describing the temporal evolution,

$$K(x'', x'; t) = \langle x''|e^{-iHt/\hbar}|x'\rangle. \tag{12}$$

According to the Feynmann's path integrals, propagator can be expressed as

$$K(x'', x'; t) = \int_{x(0)=x'}^{x(t)=x''} D[x]\exp\{(i/\hbar)W[x]\}, \tag{13}$$

where L is the Lagrangian,

$$W[x] = \int_0^t L(x, \dot{x})dt. \tag{14}$$

K can be also represented as:

$$K(x'', x'; t) = \lim_{N\to\infty}[mN/(2\pi i\hbar t)]^{dN/2}$$
$$\int_{-\infty}^{\infty}\cdots\int_{-\infty}^{\infty}\prod_{i=1}^{N-1} dx_i \exp\{\frac{i}{\hbar}\frac{t}{N}\sum_{i=1}^{N}[\frac{m}{2}(\frac{x_i - x_{i-1}}{t/N})^2 - V(x_i)]\} \tag{15}$$

In the semi-classical limit ($\hbar \to 0$), we may count only the contribution around the saddle point,

$$\delta W[x] = 0 . \tag{16}$$

Fluctuation around the saddle point can be expressed as

$$K_{scl}(x'',x',t) = (2\pi i\hbar)^{-d/2} \sum_j \sqrt{T_j} \exp\{iW_j/\hbar - i\mu_j\pi/2\} . \tag{17}$$

j is the classical trajectory originates from x(0)=x' and ends at x(t)=x", and T_j is the periodicity,

$$T_j = \left| \det(-\partial^2 W_j / \partial x'' \partial x') \right| . \tag{18}$$

μ_j is the Morse Maslov index (number of singular point between x' and x").

Laplace transformation of the propagator K is equal to the Green function,

$$G_{scl}(x'',x';E) = (i\hbar)^{-1} \int_0^\infty dt K_{scl}(x'',x';t) e^{-iEt/\hbar} . \tag{19}$$

In a stationary phase approximation,

$$G_{scl}(x'',x',t) = 2\pi(2\pi i\hbar)^{-(d+1)/2} \sum_j \sqrt{|\hat{T}_j|} \exp\{iS_j(x'',x';E)/\hbar - i\mu_j\pi/2\} \tag{20}$$

$$\hat{T}_j = \hat{T}_j(x'',x';E) = (\partial^2 W_j/\partial t^2)^{-1} \det(-\partial^2 W_j/\partial x''\partial x')\big|_{t=t_0} \tag{21}$$

$S_j(x'',x';E)$ is the reduced action obtained by the Legendre transformation of the action W_j,

$$S_j(x'',x';E) = W(x'',x';t_0) + Et_0 = \int_{x'}^{x''} p(x,E)dx \tag{22}$$

Using the basic relations in the analytical mechanics,

$$\partial W/\partial t = -E, \partial S/\partial E = t, \partial^2 W/\partial t^2 = -\partial E/\partial t = -(\partial^2 S/\partial E^2)^{-1} \tag{23}$$

$$\hat{T}_j(x'',x';E) = (-1)^d (\partial^2 S_j/\partial E^2) \det(-\partial^2 W_j/\partial x''\partial x')\big|_{t=t_0}$$

$$= \begin{vmatrix} \dfrac{\partial^2 S_j}{\partial x'\partial x''} & \dfrac{\partial^2 S_j}{\partial x'\partial E} \\ \dfrac{\partial^2 S_j}{\partial E\partial x''} & \dfrac{\partial^2 S_j}{\partial E^2} \end{vmatrix} , \tag{24}$$

which is the determinant of the (d+1) x (d+1) matrix.

$$TrG_{scl}(E) = 2\pi(2\pi i\hbar)^{-(d+1)/2}$$
$$\sum_j \int dx \sqrt{|\hat{T}_j|} \exp\{iS_j(x,x;E)/\hbar - i\mu_j\pi/2\} \tag{25}$$

In case of integrable system, the phase space is occupied by the torus and the action integral of the d closed trajectories is;

$$S_k = \oint_{\Gamma_k} ydx, (k = 1,2,\cdots d). \tag{26}$$

Thus effective action is described by the sum of the winding number l_k times S_k.

$$TrG_{scl}(E) \equiv V \sum_{l_1=0}^{\infty} \cdots \sum_{l_d=0}^{\infty} \prod_{k=1}^{d} \exp[il_k(S_k/\hbar - \mu_k\pi/2)])$$
$$= V \prod_{k=1}^{d} (1 - \exp[i(S_k/\hbar - \mu_k\pi/2)])^{-1} \tag{27}$$

μ_k is the Morse-Maslov index number and V is the d-dimensional volume. By counting only the contributions from the poles,

$$\frac{1}{2\pi}\oint_{\Gamma_k} y(E)dx = (n_k + \mu_k/4)\hbar, (n_k = 0,1,2,\cdots). \tag{28}$$

This is the Einstein-Brillouin-Keller (EBK) quantization rule.

However, in case of non-integrable system, if saddle point approximation is applicable,

$$\partial S(x,x)/\partial x \equiv \partial S(x'',x')/\partial x'' + \partial S(x'',x')/\partial x'|_{x''=x'=x} = y''-y' = 0. \tag{29}$$

The conditions, i.e. y"=y' and x"=x'=x indicate that only the periodic orbital contribute to $TrG_{scl}(E)$. Although the measure of the periodic orbital is zero, its number is infinite. Therefore, $TrG_{scl}(E)$ is represented by the sum of the periodic orbital (semi-classical quantization). Jacobian is rewritten by the global characteristics of the periodic orbital.

Let us introduce the local coordinate with the component along the periodic orbital, $x_{//}$ and those perpendicular to it, $x_{\perp}$,

$$x = (x_{//}, x_{\perp 1}, x_{\perp 2}, \cdots, x_{\perp(d-1)}) = (x_{//}, x_{\perp}). \tag{30}$$

According to the energy conservation law in the Hamilton-Jacobi equation,

$$H(x,y) = H(x, \partial S/\partial x) = E, |\partial^2 S/\partial x'\partial x''| = 0. \tag{31}$$

Therefore,

$$\hat{T}_{po} = -\frac{\partial^2 S_{po}}{\partial E \partial x_{//}''} \frac{\partial^2 S_{po}}{\partial E \partial x_{//}'} \left| \frac{\partial^2 S_{po}}{\partial x_{\perp}' \partial x_{\perp}''} \right| = (-1)^d \frac{1}{\dot{x}_{//}' \dot{x}_{//}''} \det\left(\frac{\partial y_{\perp}'}{\partial x_{\perp}''}\right) \tag{32}$$

$$S(x'',x',E)\big|_{q''=q'=q} = S_{po}(E) + (1/2)\sum_{i,j=1}^{d-1} R_{ij}(x_{//})x_{\perp i}x_{\perp j} \tag{33}$$

$S_{po}(E)$ is the action on the periodic orbital,

$$S_{po}(E) = \oint_{po} y dx \tag{34}$$

$$R(x_{//}) = \left(\frac{\partial^2 S}{\partial x_\perp'' \partial x_\perp''} + \frac{\partial^2 S}{\partial x_\perp'' \partial x_\perp'} + \frac{\partial^2 S}{\partial x_\perp' \partial x_\perp''} + \frac{\partial^2 S}{\partial x_\perp' \partial x_\perp'} \right)_{x''_\perp = x'_\perp = 0} \tag{35}$$

The contribution of each periodic orbital onto the Green function is;

$$\delta Tr G_{scl}(E) \propto \exp\{-i(S_{po}/\hbar - \mu_{po}\pi/2)\}$$
$$\int |\hat{T}_{po}(x_{//})|^{1/2} |\det R(x_{//})|^{-1/2} dx_{//} \tag{36}$$

μ_{po} is the generalized Morse-Maslov index, which includes also negative eigenvalues of $R(x_{//})$.

By use of the linearized Poincare map, i.e. monodoromy matrix, we can rewrite the above integral. Using the relationship, $\partial S/\partial x'' = y''$, $\partial S/\partial x' = -y'$, $\det R(q_{//})$ can be rewritten,

$$\begin{aligned} \det R(x_{//}) &= \det\left(\frac{\partial y_\perp''}{\partial x_\perp''} - \frac{\partial y_\perp'}{\partial x_\perp''} + \frac{\partial y_\perp''}{\partial x_\perp'} - \frac{\partial y_\perp'}{\partial x_\perp'} \right)_{x_\perp''=x_\perp'=0} \\ &= -\det\left(\frac{\partial(y_\perp''-y_\perp', x_\perp''-x_\perp')}{\partial(x_\perp''-x_\perp')} \right)_{x_\perp''=x_\perp'=0} \end{aligned} \tag{37}$$

On the other hand,

$$|\hat{T}_{po}(x_{//})| = \frac{1}{\dot{x}_{//}^{\,2}} \left| \frac{\partial y_\perp'}{\partial x_\perp''} \right|_0 = \frac{1}{\dot{x}_{//}^{\,2}} \left| \frac{\partial(y_\perp', x_\perp')}{\partial(x_\perp'', x_\perp')} \right|_0 \tag{38}$$

0 means $x_\perp' = x_\perp'' = 0$.

$$|\hat{T}_{po}(x_{//})|^{-1/2} |\det R(x_{//})|^{1/2} = |\dot{x}_{//}| \times \left| \frac{\partial(x_\perp''-x_\perp', y_\perp''-y_\perp')}{\partial(x_\perp', y_\perp')} \right|_0 \tag{39}$$

Here we introduce the 2(d-1) dimensional vector $\xi_\perp = (x_\perp, y_\perp)$, and the last term can be rewritten using the monodoromy matrix M_{po} of 2(d-1) x 2(d-1) dimensional periodic trajectory,

$$\left| \frac{\partial(x_\perp''-x_\perp', y_\perp''-y_\perp')}{\partial(x_\perp', y_\perp')} \right|_0 = \left| \frac{\partial(\xi_\perp''-\xi_\perp')}{\partial \xi_\perp'} \right|_0 = |\det(M_{po} - I)| \tag{40}$$

Therefore, when if we take into account,

$$\int \frac{1}{\dot{x}_{//}} dx_{//} = \int_p dt = T_p \,, \tag{41}$$

$TrG_{scl}(E)$ can be represented by the global characteristics of each periodic trajectory. Individual periodic trajectory is composed of prime periodic orbital or arbitrary natural number of the prime orbital. T_p is the period of p. If we can sum up all the contribution from the periodic trajectory, we can calculate TrG_{scl}. Here we consider that the unstable periodic orbital can be decomposed into the prime periodic orbital p and the natural number l_p. Action on p and period are represented by $S_p(E)$ and $T_p(E)$, respectively. Then, we can obtain the following Gutzwiller's trace formula,

$$TrG_{scl}(E) - TrG_0(E) = (i\hbar)^{-1} \sum_p T_p \sum_{l_p=1}^{\infty} \{\det(M_p^{l_p} - I)\}^{-1/2} \tag{42}$$

$$\exp\{il_p(S_p/\hbar - \mu_p \pi/2)\} + O(\hbar^0)$$

$$TrG_0(E) = (\pi/i)(2\pi\hbar)^{-d} \iint dydx\,\delta(H(x,y) - E) + O(\hbar^{-d+1}) \tag{43}$$

Monodoromy matrix describes the time evolution of the derivatives perpendicular to the trajectory $\delta x_{-}^{(n)}$. Eigenvalues of M_p, Λ_p depend on the type of fixed points. $\Lambda_p = \exp(\pm u_p)$, and $\exp(iu_p)$ for unstable and stable orbital, respectively. Especially, monodromy matrix for the homoclinic orbital with hyperbolic fixed points is, using Lyapunov index u_p (>0),

$$\det(M_p^l - I) = 4\sinh^2(lu_p/2) \tag{44}$$

If we modify the above equation using

$$[2\sinh(lu_p/2)]^{-1} = \sum_{k=0}^{\infty} \exp[-l(k+\frac{1}{2})u_p]\,. \tag{45}$$

$$TrG_{scl}(E) - TrG_0(E) \cong -\frac{d}{dE} \ln \zeta(E)\,, \tag{46}$$

where ζ (E) is the Ruelle dynamical zeta function.

$$\zeta(E) = \prod_p \prod_{k=0}^{\infty} (1 - t_p \Lambda_p^{-k})^{-1} \qquad \text{and} \qquad \text{weight}$$

$$t_p = |\Lambda_p|^{-1/2} \exp[i(S_p/\hbar - \mu_p \pi/2)]\,. \tag{47}$$

Dynamical susceptibility can be formulated using the trace formula [11],

$$\chi'' = -\frac{\omega}{2\pi}\int dt \int \frac{d^f x d^f y}{(2\pi\hbar)^f}\delta(E-H)A_W(x,y)[e^{(i\omega-\hat{L}_{cl})t}B_w](x,y)+0(\hbar^{-f+1})$$

$$-\frac{\omega}{2\pi\hbar}\delta(E_F-H)\sum_{p,r}\frac{\cos(\frac{r}{\hbar}S_p - r\frac{\pi}{2}\upsilon_p)}{\left|\det(m_p^r - I)\right|^{1/2}}\int dt e^{i\omega t}\oint_p d\tau A_W(\tau)B_W(t+\tau)+0(\hbar^0)$$

$$\cong A - \frac{d}{ds}\ln\varsigma(s)\int dt e^{i\omega t}\oint_p d\tau A_W(\tau)B_W(t+\tau)+0(\hbar^0)$$

$$\cong A - B\frac{\varsigma'(s)}{\varsigma(s)}$$

, (48)

where f is the degrees of freedom, L_{cl} is the Liouvillian operator, S_p is the action, ν_p is the Maslov index, m_p is the monodromy matrix for the periodic orbit p, and r denotes the repetition number.

The equality of periodic orbital sum and the Riemann ζ function is proved as follows:

Riemann staircase function is defined as follows;

$$N(\omega) = \sum_{K=1}^{\infty}\Lambda(\omega-\omega_k). \tag{49}$$

Oscillating part of the Riemann staircase function is described as follows;

$$N_{osc}(\omega) = -\frac{1}{\pi}\lim_{\eta\to\infty}\mathrm{Im}\ln\zeta(\frac{1}{2}-i(\omega+i\eta))$$

$$= -\frac{1}{\pi}\mathrm{Im}\sum_p\sum_{m=1}^{\infty}\frac{1}{mp^{\frac{m}{2}}}e^{i\omega m\ln(p)} \tag{50}$$

Spacing between Riemann zeros is

$$\rho_{osc} = \frac{dN_{osc}}{d\omega} = \frac{d\ln\zeta}{d\omega} = -\frac{1}{\pi}\mathrm{Im}\,g(\omega), \tag{51}$$

where

$$g(\omega) = i\sum_p\sum_{m=1}^{\infty}\frac{\ln(p)}{p^{\frac{m}{2}}}e^{iwm\ln(p)}. \tag{52}$$

While Gutzwiller's periodic orbit sum is

$$\rho_{osc}(E) = -\frac{1}{\pi}\mathrm{Im}\sum_{po} A_{po} e^{iS_{po}} \tag{53}$$

By comparing eq. 52 and 53, we can speculate as follow,

$$A_{pm} = i\frac{\ln(p)}{p^{\frac{m}{2}}},\ S_{pm} = m\omega\ln(p)\,. \tag{54}$$

Or by comparing eq.52 and 42,

$$T_p \sim \ln(p),\ \det(M_p^m - 1) \sim p^m,\ im(\frac{S_p}{\hbar} - \mu_p\frac{\pi}{2}) \sim i\omega m\ln(p) \tag{55}$$

According to E. C. Titchmarsh [12],

$$\frac{\varsigma'(s)}{\varsigma(s)} = b - \frac{1}{s-1} - \frac{1}{2}\frac{\Gamma'(1+s/2)}{\Gamma(1+s/2)} + \sum_{\mathrm{Im}\,\rho<0}(\frac{1}{\rho}+\frac{1}{\rho^*}+\frac{1}{s-\rho}+\frac{1}{s-\rho^*})$$

$$\cong -\frac{1}{1/4+\omega^2} + \frac{1}{2}\sum_{\omega_\rho>0}(\frac{1}{(1/4)^2+(\omega+\omega_\rho)^2}+\frac{1}{(1/4)^2+(\omega-\omega_\rho)^2}) \tag{56}$$

Dynamic susceptibility is usually represented using the transverse relaxation time:

$$\chi'' = \frac{\gamma M_0}{2V}\frac{T_2}{1+(\omega-\omega_0)^2T_2^2} \tag{57}$$

Thus, we can essentially evaluate the transverse relaxation times in terms of the periodical orbitals of the nuclei using the Ruelle's dynamical zeta function. Using known Riemann's zero points, we evaluated eq. 56, as shown in Fig. 1. Fig. 1 illustrates the behavior of the susceptibility as a function of frequency of periodical orbitals of nuclear spins, which is essentially independent of the nuclear magnetic resonance frequency.

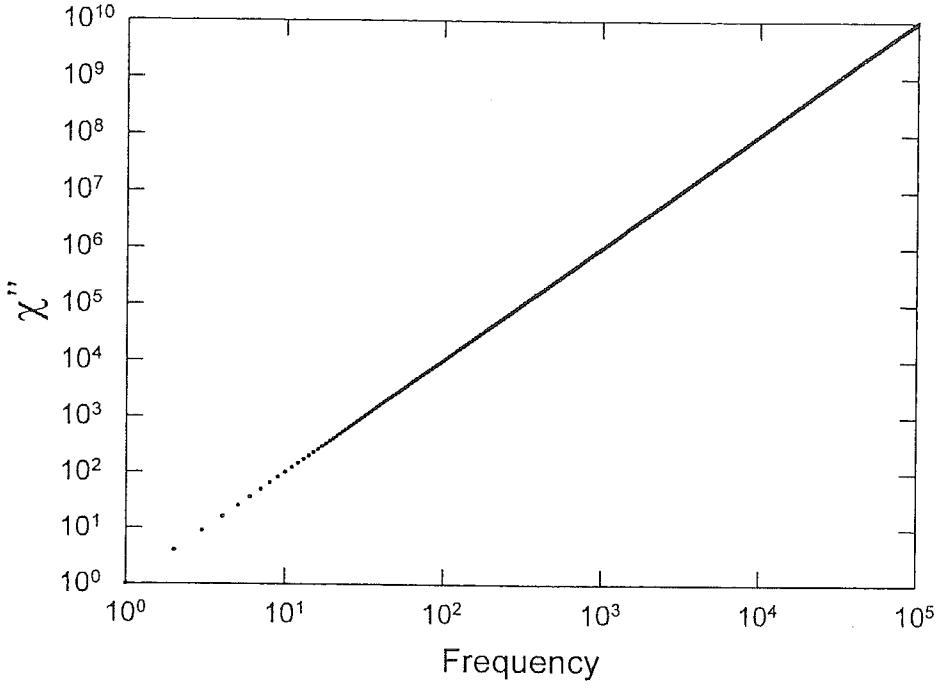

Fig. 1. A profile of susceptibility as a function of the frequency of periodical orbitals of nuclear spins, calculated using eq. 56 and known Riemann zeros.

Hecke algebraic representation of the Mori's continued fraction expansion [13]

Generalized Langevin equation (GLE) can be rewritten as follows;

$$\frac{dA(t)}{dt} = i\omega_0 A(t) - \int_0^t d\tau M(\tau) A(t-\tau) + f_1(t) \tag{58}$$

Using the following relations,

$$f_0(t) \equiv A(t), L_0 \equiv L, \Sigma_0 \equiv \Sigma(t) \equiv (f_0 \mid f_0)^{-1}(f_0 \mid f_0(t)) \tag{59}$$

$$\frac{d\Sigma_0(t)}{dt} = i\omega_0 \Sigma_0(t) - \delta_1 \int_0^t d\tau \Sigma_1(\tau)\Sigma_0(t-\tau), \tag{60}$$

where

$$\delta_1 \equiv (f_0 \mid f_0)^{-1}(f_1 \mid f_1), \Sigma_1(t) \equiv (f_1 \mid f_1)^{-1}(f_1 \mid f_1(t)). \tag{61}$$

Using the Laplace transformation, we can obtain

$$\Sigma_0(z) = [z - i\omega_0 + \delta_1 \Sigma_1(z)]^{-1} \tag{62}$$

.
.
.

$$\Sigma_j(z) = [z - i\omega_j + \delta_{j+1}\Sigma_{j+1}(z)]^{-1} \tag{63}$$

Thus

$$\Sigma_0(z) = \cfrac{1}{z - i\omega_0 + \cfrac{\delta_1}{z - i\omega_1 + \cfrac{\delta_2}{z - i\omega_2 + \cfrac{\delta_3}{z - i\omega_3 + \ldots}}}} = \tag{64}$$

$$\cfrac{1}{z - i\omega_0 + \cfrac{1}{\cfrac{z - i\omega_1}{\delta_1} + \cfrac{1}{\cfrac{z - i\omega_2}{\delta_1\delta_2} + \cfrac{\delta_3}{z - i\omega_3 + \ldots}}}}$$

Here we define

$$k_i = \frac{z - i\omega_i}{\delta_1\delta_2\cdots\delta_i} \tag{65}$$

$$p_n = [k_0, k_1, \cdots, k_{n-1}] \tag{66}$$

$$q_n = [k_1, k_2, \cdots, k_{n-1}], \tag{67}$$

where

$$[k_0] = k_0, [k_0, k_1] = k_0k_1 + 1, \cdots,$$
$$[k_0, k_1, \cdots, k_n] = [k_0, k_1, \cdots, k_{n-1}]k_{n-1}[k_0, k_1, \cdots, k_{n-2}]. \tag{68}$$

Then, Mori's equation forms modular group in this point of view, since

$$p_nq_{n-1} - p_{n-1}q_n = (-1)^n \tag{69}$$

In other words,

$$M(n) = \left\{ z \to \frac{az + b}{cz + d} : ad - bc = n; a, b, c, d \in Z \right\} \tag{70}$$

Also we can take

$$M(n) = \left\{ z \to \frac{az + b}{d} : ad = n; a, b, d \in Z \right\} \tag{71}$$

Then we can define Hecke operator,

$$(T(n)f)(z) = n^{-\frac{1}{2}} \sum_{ad=nb} \sum_{\bmod d} f\left(\left(\frac{az + b}{d}\right)\right) \tag{72}$$

It forms the Hilbert Space and we can define the Hecke eigenvalue,

$$T(n)\psi_j = t_j(n)\Psi_j \tag{73}$$

and Hecke L-fucntion which is analogous to Riemann ξ function.

$$H_j(s) = \sum_{n=1}^{\infty} t_j(n) n^{-s} = \prod_p (1 - t_j(p) p^{-s} + p^{-2s})^{-1} \tag{74}$$

where t_j is the Hecke eigenvalue. According to the above procedures, we can deal with the Langevin modes similar to the quantum mechanics in a Hilbert space, using a number theoretical technique in a framework of Hecke algebra.

Experimental results

By nuclear magnetic relaxation measurements of proteins using high resolution NMR at various nuclear magnetic resonance frequencies, we may be able to verify the above theoretical results especially represented by eq. 56 and Fig. 1. We used $p8^{MTCP1}$ as an example of thermodynamically stable globular protein [14], since the standard R1, R2 and NOE at various nuclear magnetic resonance frequencies were reported in detail. They used the model-free system for the calculation of slow exchange rate constant, Rex [10]. Briefly, R1, R2 and NOE were measured. Correlation times of the fast side chain motion (picoseconds time scale) and that of the overall tumbling motion (nanoseconds time scale) were estimated from R1 and NOE data. The contributions of these fast modes are subtracted from the R2 data. Since R2 parameter essentially includes the contribution of the slow exchange dynamics, experimentary obtained R2 minus predected R2 using the above dynamical information could be interpreted as Rex. Therefore the obtained Rex is rather conventional parameter. However, as shown in Fig. 2, nuclear magnetic resonance frequency dependencies of Rex in $p8^{MTCP1}$ were rather uniform and similar for almost all residues.

This phenomenon is reasonable, because Rex must be proportional to the square of the nuclear magnetic resonance frequency deviation, i.e. amplitude of the chemical shift deviation. Although this behavior is not contradictory to the periodic orbit approximation, the above representation must be verified further.

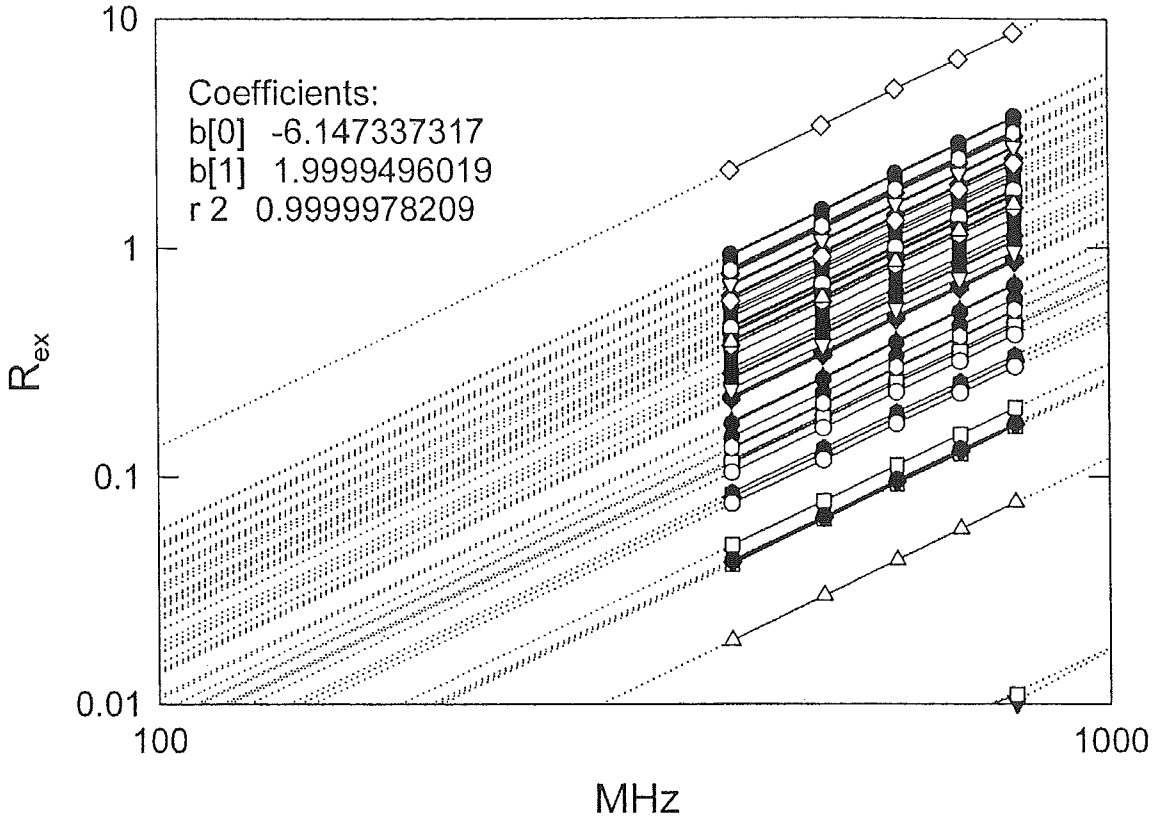

Fig. 2. Experimentally obtained Rex for $p8^{MTCP1}$ as a function of nuclear magnetic resonance frequency (^1H). All the amide nitrogen atoms showed quite similar behavior. Rex values were obtained by the model free analysis.

On the other hand, nuclear magnetic resonance frequency dependencies of Rex for prions obtained by CPMG relaxation dispersion methods [4,5] were somewhat different than those of $p8^{MTCP1}$, as shown in Fig. 3.

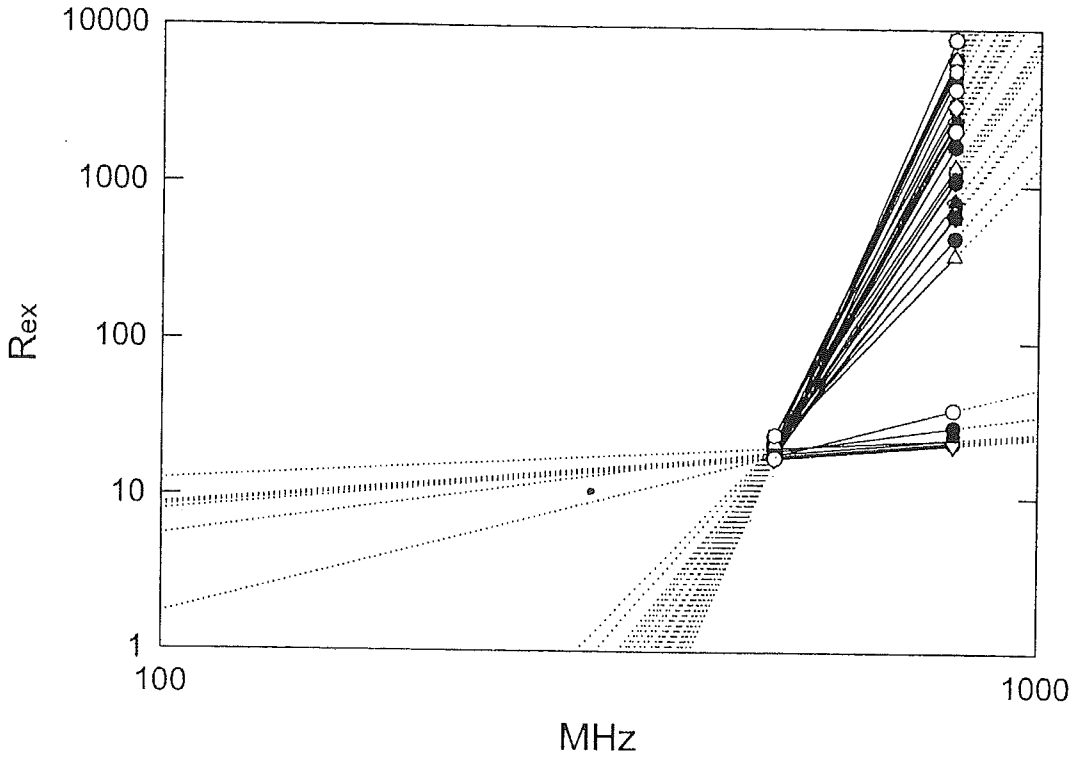

Fig. 3. Experimentally obtained Rex for hamster prion as a function of the nuclear magnetic resonance frequency (^{1}H). Amide nitrogen atoms exhibited quite heterogeneous behavior. Here Rex were estimated using CPMG relaxation dispersion methods, since model free analysis was not applicable to prion proteins [5].

They were essentially heterogeneous and seemed to be roughly categorized into two groups. Although physical details are still unknown, we may assume that the geometry of phase space around the native conformer of prion cannot be represented by a unique saddle point.

Dynamics Based Drug Design (DBDD)

We already found that the hamster prion has a folding intermediate, and residues with low stabilities undergo very slow fluctuations on a time scale of micro- to milliseconds [5]. Furthermore, distribution of residues with low stabilities corresponds to that of the causative mutations. Therefore in case of hamster prion, thermodynamical instabilities may be directly related to the initial conformational conversion process. Or thermodynamic fluctuation occurs along the trajectory between the normal to pathogenic conformation on a timescale of micro- to milliseconds.

Based on this assumption, we can design the anti-prion agents as the therapeutics quite logically using *in silico, ex vivo* and *in vivo* screening. We designated this strategy as "Dynamics Based Drug Design (DBDD)".

More than 1000 severe diseases including neurodegenerative diseases, cancer, collagen diseases, enzyme deficiency involve more or less protein structural abnormalities or thermo-dynamical instabilities. DBDD is the completely novel strategy to connect the number theory, the structural biology, and the drug discovery in the 21st century.

References

1. Sakmann B, Neher E (1983) Single channel recording, Plenum, New York
2. Harada Y, Noguchi A, Kishino A, Yanagida T (1987) Sliding movement of single actin filaments on one-headed myosin filaments. Nature 326: 805-8
3. Korzhnev D M, Salvatella X, Vendruscolo M, et al. (2004) Low-populated folding intermediates of Fyn3 SH3 characterized by relaxation dispersion NMR. Nature 430: 586-690
4. Kuwata K, Kamatari Y-O, Akasaka, K. et al. (2004) Slow conformational dynamics in the hamster prion protein. Biochemistry 43: 4439-4446
5. Kuwata K, Li H., Yamada H et al. (2002) Locally disordered conformer of the hamster prion protein: A crucial intermediate to PrP^{Sc} ? Biochemistry, 41: 12277-12283
6. Wildegger G, Liemann S, Glockshuber R. (1999) Extremely rapid folding of the C-terminal domain of the prion protein without kinetic intermediates. Nat. Struct. Biol.: 6: 550-553
7. Braxenthaler M, Unger R, Auerbach D. Given J A, Moult J (1997) Chaos in protein dynamics. Proteins 29: 417-25
8. Kubo, R., Tomita, K. (1954) A general theory of magnetic resonance absorption. J. Phys. Soc. Japan 9:888-919
9. Redfield, A. G. The Theory of relaxation processes. (1965) Adv. Mag. Reson. 1:1
10. Lipari G, Szabo A (1982) Model-free approach to the interpretation of nuclear magnetic resonance relaxation in macromolecules. 1. theory and range of validity. J. Am. Chem. Soc. 104: 4546-4559
11. Jain S R, Pati A K (1998) Adiabatic geometric phases and response functions. Phys. Rev. Lett. 80:650-653
12. Titchmarsh E C (1986) The theory of Riemann zeta function. Clarendon Press, Oxford
13. Mori H (1965) A continued-fraction representation of the time-correlation functions. Prog. Theoret. Phys. 34: 399-416
14. Canet D, Barthe P, Mutzenhardt P et al. (2001) A comprehensive analysis of multified ^{15}N relaxation parameters in proteins: Determination of ^{15}N chemical shift anisotropies. J. Am. Chem. Soc. 123: 4567-4576

JOURNAL OF VIROLOGY, June 2005, p. 7104–7112
0022-538X/05/$08.00+0 doi:10.1128/JVI.79.11.7104–7112.2005
Copyright © 2005, American Society for Microbiology. All Rights Reserved.
Vol. 79, No. 11

Biological and Biochemical Characteristics of Prion Strains Conserved in Persistently Infected Cell Cultures

Kazuhiko Arima,[1] Noriyuki Nishida,[1] Suehiro Sakaguchi,[1,3] Kazuto Shigematsu,[2] Ryuichiro Atarashi,[1] Naohiro Yamaguchi,[1] Daisuke Yoshikawa,[1] Jaewoo Yoon,[1] Ken Watanabe,[1] Nobuyuki Kobayashi,[1] Sophie Mouillet-Richard,[4] Sylvain Lehmann,[5] and Shigeru Katamine[1]*

Department of Molecular Microbiology and Immunology,[1] and Department of Pathology 2,[2] Nagasaki University Graduate School of Biomedical Sciences, Sakamoto 1-12-4, Nagasaki 852-8523, Japan; PRESTO, Japan Science and Technology Agency, 4-1-8 Honcho Kawaguchi, Saitama, Japan [3]; Institut André Lwoff, CNRS UPR 1983-BP8, 94801 Villejuif Cedex, France[4]; and Institut de Genetique Humaine, CNRS UPR 1142, 34396 Montpellier Cedex 5, France[5]

Received 16 August 2004/Accepted 18 January 2005

Abnormal prion protein (PrP^{Sc}) plays a central role in the transmission of prion diseases, but the molecular basis of prion strains with distinct biological characteristics remains to be elucidated. We analyzed the characteristics of prion disease by using mice inoculated with the Chandler and Fukuoka-1 strains propagated in a cultured mouse neuronal cell line, GT1-7, which is highly permissive to replication of the infectious agents. Strain-specific biological characteristics, including clinical manifestations, incubation period as related to the infectious unit, and pathological profiles, remained unchanged after passages in the cell cultures. We noted some differences in the biochemical aspects of PrP^{Sc} between brain tissues and GT1-7 cells which were unlikely to affect the strain phenotypes. On the other hand, the proteinase K-resistant PrP core fragments derived from Fukuoka-1-infected tissues and cells were slightly larger than those from Chandler-infected versions. Moreover, Fukuoka-1 infection, but not Chandler infection, gave an extra fragment with a low molecular weight, ~13 kDa, in both brain tissues and GT1-7 cells. This cell culture model persistently infected with different strains will provide a new insight into the understanding of the molecular basis of prion diversity.

Transmissible spongiform encephalopathies (TSEs) are a series of neurodegenerative disorders that include Creutzfeldt-Jakob disease (CJD), Gerstmann-Straussler-Scheinker syndrome (GSS), and fatal familial insomnia in humans and bovine spongiform encephalopathy and scrapie in animals (23, 25). Human TSEs may have infectious, sporadic, or genetic origins, but the brain tissues from affected individuals always possess an infectious agent, termed prion, capable of transmitting the disease to laboratory animals. The protein-only hypothesis proposes that the abnormal isoform of the prion protein (PrP^{Sc}) accumulated via posttranslational modification of the cellular isoform (PrP^{C}) is the sole component of the infectious particle (25). In fact, while the agent is extremely resistant to inactivation by UV and ionizing radiation, protein denaturants can abolish the infectivity, and moreover, no specific genetic materials for infectious agents have been identified. The two PrP isoforms are distinguishable by their biochemical properties. PrP^{C} is readily soluble in nondenaturing detergents and completely digested by proteinase K (PK), whereas PrP^{Sc} is detergent insoluble and resistant to proteolysis except for the N-terminal region comprising ~67 residues. Structural studies have suggested that the former is rich in alpha-helical structures with small β-sheet regions, but the latter has a high β-sheet content. The central role of PrP in the diseases is exemplified by the fact that PrP-null mice are resistant to the disease (6, 27), by the causal linkage of genetic forms of human TSEs with mutation in the PrP gene (25), and by the dependency of the species barriers on the primary PrP sequences (29). The existence of strain variation, however, has challenged the protein-only hypothesis. Individual infectious agents have been shown to maintain their phenotypic characteristics, including the clinical presentation of disease, the length of the incubation period, and the distribution of vacuolar degeneration and PrP^{Sc} deposition in the central nervous system (CNS) during serial transmission between same-species animals. In addition to these biological characteristics, biochemical differences in PrP^{Sc} have been reported. Transmission of two different inherited human prion diseases, fatal familial insomnia and familial CJD, to mice resulted in the accumulation of PrP^{Sc} with PK-resistant core fragments with molecular masses of 19 and 21 kDa, respectively (35). The difference in the size of PK-resistant PrP^{Sc} fragments has been also documented among agents originating from scrapie and mink spongiform encephalopathies (3). The degree of glycosylation is also proposed to be an important signature of some strains. There are two sites of Asn-linked glycosylation at the C-terminal portion, and the degree of glycosylation is thus represented by the ratio of three glycoforms, di-, mono-, and unglycosylated forms. The unique PrP^{Sc} glycoform pattern, in which the diglycosylated form dominates, in animals and patients affected with bovine spongiform encephalopathy and variant CJD, respectively, is distinct from those of other known strains (11) with a few exceptions (32). Because diversity in the size of a PK-resistant PrP core fragment and the degree of its Asn-linked glycosylation were thought to be consequences of differences in the conformation, it has been hypothesized that strain-specific conformations of PrP^{Sc} could determine the strain phenotype.

* Corresponding author. Mailing address: Department of Molecular Microbiology and Immunology, Nagasaki University Graduate School of Biomedical Sciences, Sakamoto 1-12-4, Nagasaki 852-8523, Japan. Phone: 81-95-849-7057. Fax: 81-95-849-7060. E-mail: katamine@net.nagasaki-u.ac.jp.